Attenuation of mechanical vibrations at low frequencies by a nonlinear dynamical absorber

D. LAVAZEC[a,b], G. CUMUNEL[a], D. DUHAMEL[a], C. SOIZE[b]

a. Université Paris-Est, Laboratoire Navier, ENPC/IFSTTAR/CNRS, 6 et 8 Avenue Blaise Pascal, Cité Descartes, Champs-sur-Marne, 77455 Marne La Vallée Cedex 2, France
b. Université Paris-Est, Laboratoire Modélisation et Simulation Multi Echelle, MSME UMR 8208 CNRS, 5 bd Descartes, 77454 Marne-la-Vallée, France
Email : deborah.lavazec@univ-paris-est.fr

Résumé :

À l'heure actuelle, l'atténuation des ondes acoustiques et des vibrations mécaniques en moyennes et hautes fréquences est bien connue et facilement réalisable, en particulier avec des matériaux dissipatifs. Cependant, cette atténuation est beaucoup plus difficile à réaliser en basses fréquences en raison des grandes longueurs d'onde. Dans le travail présenté ici, nous proposons de réduire et les vibrations en basses fréquences sur une large bande de fréquences au moyen d'absorbeurs non-linéaires permettant un transfert et une dissipation de l'énergie. A terme, l'objectif est de répartir aléatoirement de tels absorbeurs non linéaires dans une matrice pour atténuer les ondes acoustiques et les vibrations. L'absorbeur se compose d'une poutre console avec une masse à son extrémité. Il est conçu pour obtenir un comportement dynamique non-linéaire en basses fréquences grâce aux déplacements finis de la poutre. Ce système mécanique est modélisé par un système masse-ressort-amortisseur avec une rigidité et un amortissement non-linéaires. En effet, la non-linéarité permet une atténuation sur une bande de fréquence plus large, contrairement aux systèmes linéaires qui ne génèrent qu'une réduction sur une bande de fréquences étroite autour de la résonance, ce qui permet de réduire le nombre d'absorbeurs nécessaires pour une atténuation donnée. Nous allons d'abord présenter la conception de l'absorbeur non-linéaire optimisé en utilisant une modélisation stochastique afin d'obtenir la réponse non-linéaire la plus forte possible. Ensuite, les résultats expérimentaux seront présentés ainsi que ceux obtenus à partir du modèle proposé pour l'absorbeur.

Abstract :

At the present time, the attenuation of acoustic waves and mechanical vibrations at high and middle frequencies is well known and easily done, especially with dissipative materials. However, this attenuation is much more difficult to realize at low frequencies because of the large wavelengths. In the work presented here, we propose to reduce the vibration at low frequencies over a broad frequency band by means of nonlinear absorbers allowing a transfer and a dissipation of the energy. Ultimately, the objective is to randomly distribute such non-linear absorbers in a matrix to attenuate acoustic waves and vibrations. The absorber consists of a cantilever beam with a mass at its end. It is designed in order to obtain a nonlinear dynamical behavior at low frequencies due to the finite displacements of the beam. This mechanical system is modeled by a mass-spring-damper system with a nonlinear stiffness and a

nonlinear damping. Indeed, nonlinearity allows attenuation over a broader frequency band, than for linear systems for which the reduction only works on a narrow frequency band around the resonance, reducing the number of absorbers needed for a given attenuation . We will first present the design of the nonlinear absorber optimized using stochastic modeling in order to obtain the strongest nonlinear response possible. Then, experimental results will be presented as well as those obtained by the proposed model of the absorber.

Keywords : vibrations attenuation, nonlinear absorber, homogeneization, metamaterial

1 Introduction

As it is well known, the reduction of acoustic waves and vibration at middle and high frequencies is mainly done by dissipative materials. With these materials, waves are reduced thanks to the pores of the materials. However, for low frequencies, the wavelength are larger that the pores, and dissipative materials are less efficient. To get around this problem at low frequencies, absorbers have been designed, in particular oscillators. Among the first papers devoted to the enery pumping by simple oscillators, the work by Frahm [1] in 1911 can be cited. The author proposed the idea of adding an auxiliary body to a structure to reduce or avoid vibration due to periodic impacts. The resonance vibration of the main body is annulled by the secondary resonance vibration of the smaller auxiliary body. In nearer years, tuned mass dampers have been studied. The principle is to add an oscillator (generally a mass-spring-damper system) to a main structure with a problematic resonance. The resonance frequency of the damper is ajusted in order to be the same as the structure's to attenuate the resonance. With that, the peak is divided into two peaks of low amplitudes. A review made by Gutierrez Soto et al. [2] presents a representative research on tuned mass dampers. Metamaterials have also been used for the reduction of noise and vibration. A metamaterial is a material with properties that can not be find in nature, generally a composite. There are for instance materials with both negative permittivity and negative permeability in optics [3]. In the field of absorption of vibration and noise, numerous papers have been published with metamaterials, as for instance, [4, 5, 6, 7, 8, 9, 10, 11]. In 1952, Roberson [12] have presented the equations of a nonlinear dynamic vibration absorber and highlighted the fact that an auxiliary body with nonlinear dynamical behavior offers significant advantages over a linear absorber. This was confirmed by Soize [13] in 1995 that the transfer of the energy is done over a broader frequency band with a nonlinear auxiliary body than a linear one. Concerning the energy pumping by nonlinear mechanical oscillators in order to attenuate vibration for discrete or continuous systems at macro- or at micro-scales, many works have been published such as [14, 15, 16, 17, 18, 19, 20, 21].

This paper is devoted to the reduction of vibration in structures at macro-scale for low frequencies for which the first structural modes are excited. The final objective of this work is to reduce vibration on a broad low-frequency band by using a microstructured material by inclusions that are randomly arranged in the material matrix. The first step of this work is to design and to analyze the efficiency of an inclusion, which is made up of a cantilever beam with a mass at its end. This inclusion behaves as a nonlinear oscillator which designed so that the energy pumping is effective on a broad frequency band around its resonance instead of a narrow frequency band as for a linear oscillator. For this first step, the objective

is to develop the simplest mechanical model that has the capability to roughly predict the experimental results. The second step will consist in developing a more advanced nonlinear dynamical system. In this paper, devoted to the first step, it is proved that the nonlinearity induced an attenuation on a broad frequency band around its resonance, whereas the associated linear system applies a reduction only on a narrow frequency band. We will present the design of the inclusion in terms of form, dimension and materials, the experimental manufacturing of this system realized with a 3D printing system, and the experimental measurements that have been performed. The prevision given by the stochastic computational model are compared to the measurements. The results obtained exhibit the physical attenuation over a broad low-frequency band, which were expected.

In Section 2, the model of the inclusion and the related stochastic solver are introduced. Then, the experimental design is presented in Section 3 as well as the experimental measurements and the identification of the model. In Section 4, the conclusions on the results of this work and the perspectives of the future work are given.

2 Design of the nonlinear model and stochastic solver

2.1 Model of the inclusion

As explained in Section 1, a nonlinear oscillator with one DOF is proposed to model the nonlinear dynamical behavior of the inclusion. The one-DOF nonlinear model is composed of a mass-spring-damper system with a nonlinear spring and a nonlinear damping, subjected to base excitation (see the scheme displayed in Figure 1). Let $X_{\text{imp}}^{\text{exp}}(t)$ be the displacement imposed at the base in the absolute frame and let $X_s(t)$ be the relative displacement of the point mass with respect to the base. Let

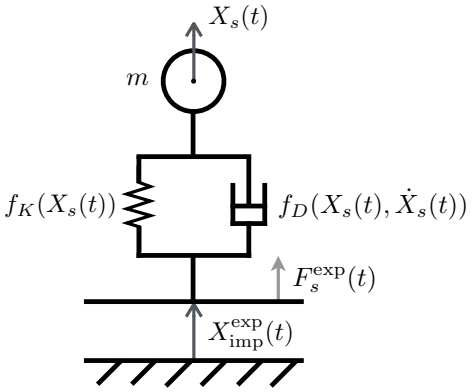

FIGURE 1 – 1D simplified model.

$\{\ddot{X}_{\text{imp}}^{\text{exp}}(t), t \in \mathbb{R}\}$ be the acceleration imposed to the base, which is a Gaussian stationary second-order centered stochastic process, defined on the probability space $(\Theta, \mathcal{T}, \mathcal{P})$, for which the power spectral density function is denoted by $S_{\ddot{X}_{\text{imp}}^{\text{exp}}}(\omega)$. We aim to find the stationary second-order stochastic solution $\{X_s(t), t \in \mathbb{R}\}$ (which is not Gaussian) of the following stochastic nonlinear equation $m(\ddot{X}_s(t) + \ddot{X}_{\text{imp}}^{\text{exp}}(t)) + f_D(X_s(t), \dot{X}_s(t)) + f_K(X_s(t)) = 0$ for t in $\mathbb{R}$, which is rewritten as

$$m\ddot{X}_s(t) + f_D(X_s(t), \dot{X}_s(t)) + f_K(X_s(t)) = F_s^{\text{exp}}(t),\ t \in \mathbb{R}, \tag{1}$$

with

$$F_s^{\text{exp}}(t) = -m\,\ddot{X}_{\text{imp}}^{\text{exp}}(t)\,,$$
$$f_D(X_s(t),\dot{X}_s(t)) = \big(c_1 + c_2|X_s(t)|\big)\dot{X}_s(t)\,,$$
$$f_K(X_s(t)) = k_1 X_s(t) + k_3(X_s(t))^3\,,$$

where m is the mass of the inclusion introduced before, c_1 and c_2 are the damping coefficients and k_1 and k_3 are the stiffness coefficients. The nonlinear stiffness is written as a cubic nonlinearity because it is the form of nonlinearity due to geometric effects that can be observed experimentally in our case. We did not add quadratic coefficient in order to obtain a centered response as the excitation is a centered stochastic process.

The mean input power $\Pi_{\text{in}} = E\{F_s^{\text{exp}}(t)\,\dot{X}_s(t)\}$ (in which E is the mathematical expectation) and the mean power dissipated $\Pi_{\text{diss}} = E\{f_D(X_s(t),\dot{X}_s(t))\dot{X}_s(t)\}$, which are independent of t and which are equal (due to the stationarity), can be written as $\Pi_{\text{in}} = \int_{\mathbb{R}} \pi_{\text{in}}(\omega)\,d\omega$ and $\Pi_{\text{diss}} = \int_{\mathbb{R}} \pi_{\text{diss}}(\omega)\,d\omega$, in which the density $\pi_{\text{in}}(\omega)$ and $\pi_{\text{diss}}(\omega)$ are such that

$$\pi_{\text{in}}(\omega) = S_{F_s^{\text{exp}}\dot{X}_s}(\omega) \quad , \quad \pi_{\text{diss}}(\omega) = S_{f_D\dot{X}_s}(\omega)\,. \tag{2}$$

In Eq. (2), $S_{F_s^{\text{exp}}\dot{X}_s}$ is the cross-spectral density function of the stationary stochastic processes F_s^{exp} and $\dot{X}_s$, and $S_{f_D\dot{X}_s}(\omega)$ is the cross-spectral density function of the stationary stochastic processes f_D and $\dot{X}_s$. The energy pumping expressed as a function of the frequency is therefore characterized by $\pi_{\text{in}}(\omega) = \pi_{\text{diss}}(\omega)$. In order to qualify the efficiency of the energy pumping as a function of the intensity of the nonlinearity, we introduce the normalized quantity,

$$\pi_{\text{in,norm}}(\omega) = \frac{\pi_{\text{in}}(\omega)}{S_{F_s^{\text{exp}}}(\omega)}\,. \tag{3}$$

Finally, the damping and stiffness coefficients will be experimentally identified by using the frequency dependent function $\text{FRF}^2(\omega)$ defined on B_0 by,

$$\text{FRF}^2(\omega) = \frac{|S_{\dot{X}_s F_s^{\text{exp}}}(\omega)|^2}{|S_{F_s^{\text{exp}}}(\omega)|^2} \tag{4}$$

It should be noted that if $f_D(x)$ and $f_K(x)$ were linear functions of x (linear oscillator), then FRF^2 would represent the square of the modulus of the frequency response function of the associated linear filter for which F_s^{exp} is the input and $\dot{X}_s$ is the output.

2.2 Stochastic solver and signal processing

Stochastic solver. For constructing the stationary stochastic solution of the nonlinear differential equation Eq. (1), the Monte Carlo method (see [22]) is used. Let $\{F_s^{\text{exp}}(t;\theta_\ell), t \in \mathbb{R}\}$ be a realization of the stochastic process F_s^{exp} for $\theta_\ell \in \Theta$. Considering L independent realizations, for each realization θ_ℓ, we

then have to solve the deterministic nonlinear differential equation with initial conditions,

$$\left\{ \begin{array}{l} m\ddot{X}(t;\theta_\ell) + f_D(X(t;\theta_\ell),\dot{X}(t;\theta_\ell)) + f_K(X(t;\theta_\ell)) = F_s^{\text{exp}}(t;\theta_\ell),\ t\in[0,t_0+T], \\ \\ X(0,\theta_\ell)=0,\ \dot{X}(0,\theta_\ell)=0. \end{array} \right. \tag{5}$$

The part $\{X(t;\theta_\ell), t\in[0,t_0]\}$ of the non-stationary random response corresponds to the transient signal induces by the initial conditions, that decreases exponentially due to the damping. This part of the response is removed in the signal analyzing of the second-order quantities of the stationary solution. Time t_0 is chosen in order that the transient response be negligible for $t \geq t_0$. The part of the trajectory corresponding to the stationary response is $X_s(t;\theta_\ell) = X(t-t_0;\theta_\ell)$ for t in $[t_0, t_0+T]$. The time duration T that is related to the frequency resolution is defined after. The deterministic problem defined by Eq. (5) will be solved with a Störmer-Verlet scheme presented after.

Time and frequency sampling. For constructing the second-order quantities of the stationary response X_s, the signal processing requires a time sampling with a constant time step Δ_t that is performed using the Shannon theorem for the stationary stochastic processes [23]. The sampling frequency is thus written as $f_e = 2\,f_{\text{max}}$ where f_{max} is the maximal frequency and the time step is $\Delta_t = 1/f_e$. The corresponding time sampling is $t_\alpha = \alpha\,\Delta_t$ with $\alpha = 0,1,...,N-1$ in which the integer N is chosen in order that the time duration is $T = 8\,s$, where $T = N\Delta_t$ yielding the frequency resolution $\Delta_f = 1/T = 0.125\,Hz$ and $N = 16,384$. The corresponding sampling points in the frequency domain are $f_\beta = -f_{\text{max}} + (\beta+1/2)\Delta_f$ for $\beta = 0,1,...,N-1$.

Generation of independent realizations of stochastic process F_s^{exp}. The usual second-order spectral representation of the stationary stochastic processes is used [24, 25]. The power spectral density function $S_{F_s^{\text{exp}}}(\omega)$ of the Gaussian stationary second-order centered stochastic process F_s^{exp} is such that $S_{F_s^{\text{exp}}}(\omega) = m^2\,S_{\ddot{X}_{\text{imp}}^{\text{exp}}}(\omega)$, in which $S_{\ddot{X}_{\text{imp}}^{\text{exp}}}(\omega) = \omega^4\,S_{X_{\text{imp}}^{\text{exp}}}(\omega)$. The autocorrelation function $\tau \mapsto R_{\ddot{X}_{\text{imp}}^{\text{exp}}}(\tau)$ of stochastic process $\ddot{X}_{\text{imp}}^{\text{exp}}$ is such that $R_{\ddot{X}_{\text{imp}}^{\text{exp}}}(\tau) = E\{\ddot{X}_{\text{imp}}^{\text{exp}}(t+\tau)\ddot{X}_{\text{imp}}^{\text{exp}}(t)\}$ and $R_{\ddot{X}_{\text{imp}}^{\text{exp}}}(\tau) = \int_R e^{i\omega\tau} S_{\ddot{X}_{\text{imp}}^{\text{exp}}}(\omega)\,d\omega$. The generator of realizations of the Gaussian stationary second-order stochastic process $\ddot{X}_{\text{imp}}^{\text{exp}}$ is based on the usual spectral representation (see [26, 27]). Let $\Psi_0,\ldots,\Psi_{N-1}$ be N mutually independent uniform random variables on $[0,1]$, and let $\phi_0,\ldots,\phi_{N-1}$ be N mutually independent uniform random variables on $[0,2\pi]$, which are independent of $\Psi_0,\ldots,\Psi_{N-1}$. The spectral representation used is,

$$\ddot{X}_{\text{imp}}^{\text{exp}}(t) \simeq \sqrt{2\Delta_\omega}\,\text{Re}\Big\{\sum_{\beta=0}^{N-1}\sqrt{S_{\ddot{X}_{\text{imp}}^{\text{exp}}}(\omega_\beta)}\,Z_\beta\,e^{-i\omega_\beta t}\,e^{-i\phi_\beta}\Big\},\ t\in[0,t_0+T]\ , \tag{6}$$

with $\Delta_\omega = 2\pi\,\Delta_f$, where $Z_\beta = \sqrt{-\log(\Psi_\beta)}$ and $\omega_\beta = 2\pi\,f_\beta$.

From Eq. (6), it can be deduced that the realization $\{\ddot{X}_{\text{imp}}^{\text{exp}}(t;\theta_\ell)\,, t\in[t_0;t_0+T]\}$ is written as

$$\ddot{X}_{\text{imp}}^{\text{exp}}(t;\theta_\ell) \simeq \sqrt{2\Delta_\omega}\,\text{Re}\Big\{\sum_{\beta=0}^{N-1} g_{\beta,\ell}\,e^{-i\omega_\beta t}\Big\},\ t\in[0,t_0+T]\,, \tag{7}$$

with $g_{\beta,\ell} = \sqrt{S_{\ddot{X}^{\exp}_{\text{imp}}}(\omega_\beta)}\, Z_\beta(\theta_\ell)\, e^{-i\phi_\beta(\theta_\ell)}$. Introducing the FFT $\{\widehat{g}_{0,\ell}, \ldots, \widehat{g}_{N-1,\ell}\}$ of $\{g_{0,\ell}, \ldots, g_{N-1,\ell}\}$, which is written as $\widehat{g}_{\alpha,\ell} = \sum_{\beta=0}^{N-1} g_{\beta,\ell}\, \exp\{-2i\,\pi\,\alpha\beta/N\}$ for $\alpha = 0, 1, ..., N-1$, we obtain

$$\ddot{X}^{\exp}_{\text{imp}}(t_\alpha;\theta_\ell) = \sqrt{2\Delta_\omega}\, \text{Re}\Big\{ \exp\big\{ -i\pi\alpha\big(\frac{1-N}{N}\big)\big\}\, \widehat{g}_{\alpha,\ell}\Big\}\,, \alpha = 0, 1, \ldots, N-1\,. \tag{8}$$

Störmer-Verlet integration scheme. The Störmer-Verlet integration scheme is well suited for the resolution of dynamical Hamiltonian systems [28, 29] as proposed, for instance, for the dissipative case in [30]. Such a scheme preserves the mechanical energy during the numerical integration. We thus rewrite Eq. (5) in the following dissipative Hamiltonian form as

$$\left\{\begin{array}{l} \dot{X}(t;\theta_\ell) = \dfrac{1}{m}\, Y(t;\theta_\ell), \qquad t \in [t_0, t_0+T]\,, \\ \\ \dot{Y}(t;\theta_\ell) = -f_D(Y(t;\theta_\ell) - k_1 X(t;\theta_\ell) \\ \qquad\qquad -k_3(X(t;\theta_\ell))^3 + F_s^{\exp}(t;\theta_\ell), \qquad t \in [t_0, t_0+T]\,, \\ \\ X(0;\theta_\ell) = 0\,,\ Y(0;\theta_\ell) = 0\,. \end{array}\right. \tag{9}$$

We use the notation $u_\ell^\alpha = U(t_\alpha;\theta_\ell)$. The Störmer-Verlet integration scheme for Eq. (9) is then written, for $\alpha = 0, 1, ..., N-1$, as

$$\left\{\begin{array}{l} x_\ell^{\alpha+1/2} = x_\ell^\alpha + \dfrac{\Delta_t}{2m}\, y_\ell^\alpha\,, \\ \\ y_\ell^{\alpha+1} = y_\ell^\alpha + \Delta_t\Big[-\dfrac{f_D(y_\ell^\alpha) + f_D(y_\ell^{\alpha+1})}{2} \\ \qquad\qquad -k_1 x_\ell^{\alpha+1/2} - k_3(x_\ell^{\alpha+1/2})^3 + F_s^{\exp}(t_{\alpha+1};\theta_\ell)\Big]\,, \\ \\ x_\ell^{\alpha+1} = x_\ell^{\alpha+1/2} + \dfrac{\Delta_t}{2m} y_\ell^{\alpha+1}\,, \end{array}\right. \tag{10}$$

in which $F_s^{\exp}(t_{\alpha+1};\theta_\ell) = -m\ddot{X}^{\exp}_{\text{imp}}(t_{\alpha+1};\theta_\ell)$.

Signal processing. For estimating, the power spectral density functions and the cross-spectral density functions defined in Eqs. (2) and (4), the periodogram method [23] is used.

3 Experimental design choice, measurements and identification of the model

In Section 2, we defined the model of the inclusion and the related stochastic solver. In this section, we want to design a experimental structure that can be assimilated to an one-DOF nonlinear oscillator.

Concerning the design of the nonlinear oscillator, we had several constraints. Indeed, the dimension of the inclusion was set at about two centimeters, in order to be of the size of the biggest aggregates

in concrete, supposing that the inclusion can be put in a wall of concrete. In addition, we wanted an oscillator with a strong nonlinear behavior without important displacements to remain in the bulk define previously. Also, we needed an oscillator with a weak damping to absorb the energy on a broad frequency band. After tests on different structures (these tests will be develop in a future paper), we chose to focus on a cantilever beam with a mass at its end.

3.1 Presentation of the test structure

The inclusion has been designed at a macro-scale ans this inclusion is manufactured using a 3D printing system. The material of the inclusion and of the frame is in ABS , which is commonly used as a material for 3D printing. It is made up of a mass constituted of a cube, embedded at the end of a beam. The other end of the beam is integral with the frame. The beam length is $0.026\,m$ and its square section is $0.001 \times 0.001\,m^2$. The exterior dimensions of the cube are $0.008 \times 0.008 \times 0.008\,m^3$. The mass m of the inclusion

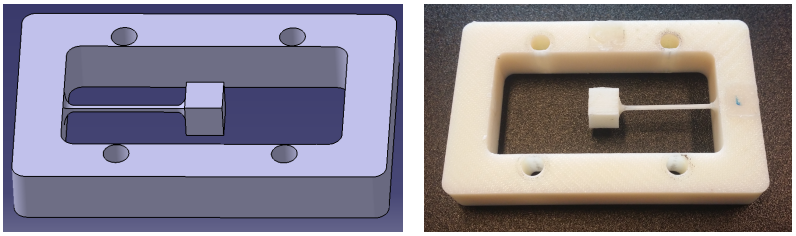

(a) CAO (b) 3D printing

FIGURE 2 – CAO and 3D printing of the test structure.

is approximated by the sum of the mass of the accelerometer attached to it for the measurements, that is $0.4\,g$, the mass of its cable $0.2\,g$ and the mass of the cube $0.55\,g$, so the mass m is $1.2\,g$ (the mass of the beam is neglected). The mass density of the ABS is $1,780\,kg/m^3$. Some experimental traction tests have been carried out to identify the mechanical properties of the ABS material. The experiments give for the Young modulus, $2.2 \times 10^9\,Pa$ and for the Poisson coefficient 0.35. This inclusion has been designed so that the first eigenfrequency of the frame be around $1,200\,Hz$ and the first eigenfrequency of the inclusion (point mass, accelerometer and beam) around $24\,Hz$. We are interested in analyzing the stationary random response of the inclusion in the frequency band of analysis $B_a = [0, f_{\text{max}}]$ with $f_{\text{max}} = 1,024\,Hz$, induced by the stationary random excitation of the embedded end of the beam. The acceleration of the base of the beam is equal to the acceleration imposed to the frame (considered as rigid in the frequency band), on which a stationary random external force is applied (see Section 3). The observed frequency band is the band $B_o = [21, 26]\,Hz$, which contains the resonance frequency for all the amplitudes of the excitation.

3.2 Experimental results and identification of the model

The experimental configuration can be viewed in Figure 3. The acceleration $\ddot{X}^{\text{exp}}_{\text{imp}}$ at a point of the rigid frame fixed to the shaker and the acceleration $\ddot{X}^{\text{exp}}_{S}$ of the mass (inclusion) are measured by two accelerometers. The excitation applied to the rigid frame is done by a shaker. The experimental responses have been measured for seven amplitude levels of the acceleration $\ddot{X}^{\text{exp}}_{\text{imp}}$. These cases are identified by the ratio d/h where h is the thickness of the beam ($h = 0.001\,m$) and d is defined as the mean of the “

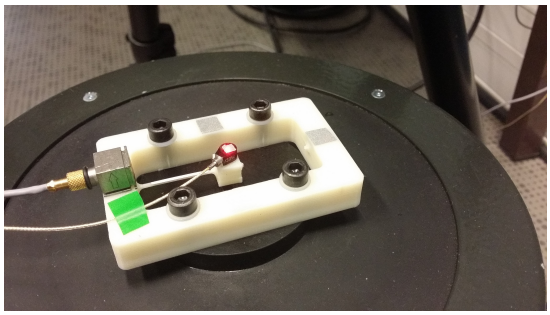

FIGURE 3 – The experimental configuration.

peak-to-peak" deflection amplitudes obtained for each measurement block :

$$d = \frac{100}{2L}\Big(\sum_{\ell=1}^{L} max(X^{\exp}(t;\theta_\ell)) - \sum_{\ell=1}^{L} min(X^{\exp}(t;\theta_\ell))\Big) \ .$$

For instance, if $d/h = 100\%$, the displacement of the inclusion is of the order of magnitude of the thickness of the beam. The power spectral density function of the force applied to the oscillator $S_{F_s}^{\exp}$ is displayed in Figure 4 for each case and for the frequency band B_o.

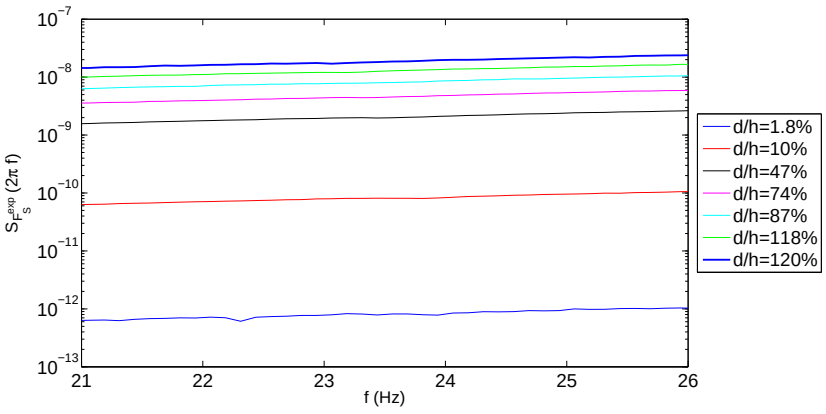

FIGURE 4 – Experimental PSD function $S_{F_x}^{exp}$ for seven amplitudes of the excitation.

As explained in Section 2.1, for all amplitudes, the experimental identification of the damping and stiffness parameters is performed by minimizing over the frequency band B_o, the distance between the function FRF^2 (Eq. (5)) computed with the model and with the experimental measurements.
During the identification process, we have noted that the damping of the system was nonlinear. According to [31], the form chosen to model the damping in order to keep a centered response is $f_D(X_s(t), \dot{X}_s(t)) = \big(c_1 + c_2|X_s(t)|\big)\dot{X}_s(t)$. The experimental identification gives for the stiffness and damping coefficients

$$\begin{cases} k_1 = 26.8\, N/m \ , \\ k_3 = -4 \times 10^6 N/m^3 \ , \\ c_1 = 0.0038\, Ns/m \ , \\ c_2 = 10\, Ns/m^2 \ . \end{cases} \tag{11}$$

For each of the seven amplitudes, Figure 5 displays the functions FRF^2 obtained by the identified model and experimentally. It can be seen a reasonable agreement between the experiments and the computation, knowing that an approximation has been introduced for constructing the model (see the explanations given in Section 2.1).

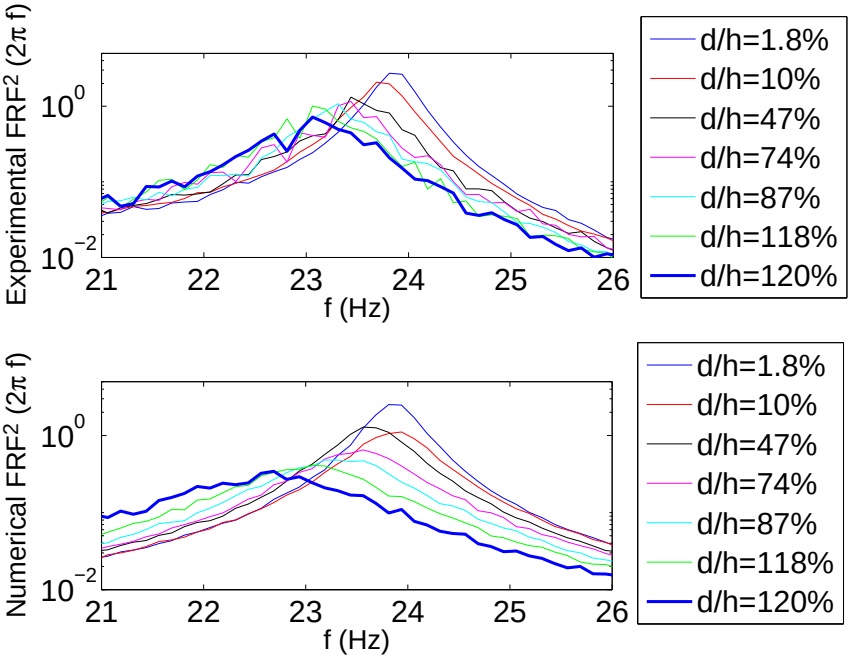

FIGURE 5 – Functions FRF^2 obtained experimentally and with the identified model for the seven amplitudes of excitation.

Figure 6 displays the experimental and numerical normalized input power density defined by Eq. (3) for seven amplitudes of excitation. A reasonable agreement can also be seen between the model prediction and the experiments. Furthermore, the results presented in this figure confirm a strong effect of the nonlinearity that allows the pumping energy phenomenon to be efficient over a broader frequency band around the resonance frequency than for the linear case, which was the objective of this study.

4 Conclusions

In this paper, we have presented the results related to the first step of a work devoted to the design and the analysis of a nonlinear microstructured material to reduce vibrations at low frequencies. We have designed an inclusion at macroscale, which has been manufactured with a 3D printing system. The dimension of this inclusion can easily be reduced with the same technology. A nonlinear dynamical model has been developed and its parameters have been identified with the experiments. Both the predictions given by the model and the experiments confirm that the pumping energy phenomenon is more efficient over a broader frequency band around the resonance frequency than for the linear case. The work in progress is the use of absorbers based on such a technologies for analyzing the attenuation of acoustics waves and vibrations in materials.

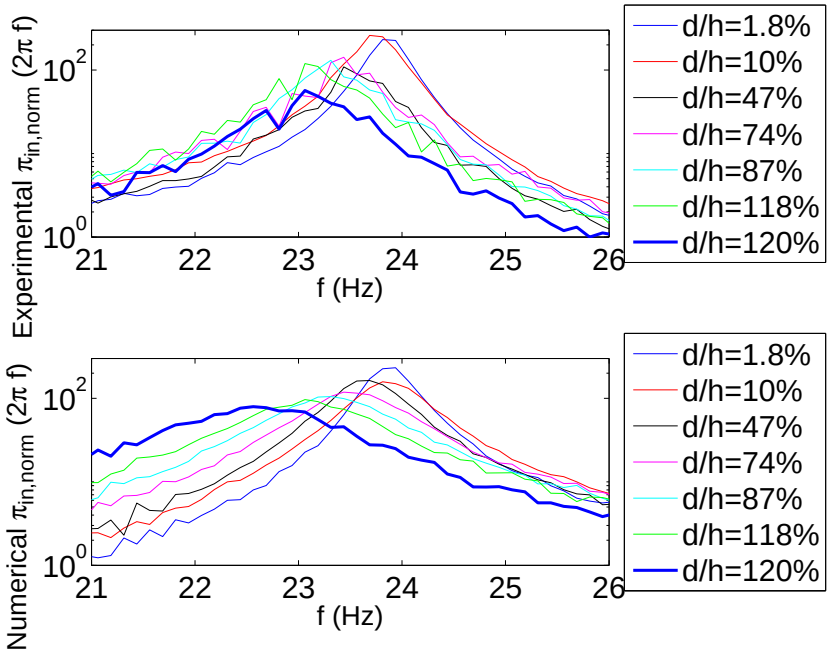

FIGURE 6 – Normalized input power density $\pi^{exp}_{\text{in,norm}}$ obtained experimentally and with the identified model for the seven amplitudes of excitation.

Acknowledgements

This work has benefited from a French government grant managed by ANR within the frame of the national program investments for the Future ANR-11-LABX-002-01.

References

[1] H. Frahm, Device for damping vibrations of bodies, United states patent office (1911) 1–9.

[2] M. Gutierrez Soto, H. Adeli, Tuned mass dampers, Archives of Computational Methods in Engineering 20 (4) (2013) 419–431.

[3] V. G. Veselago, The electrodynamics of substances with simultaneously negative values of ϵ and ν, Soviet Physics 10 (1968) 509–514.

[4] D. Smith, N. Kroll, Negative refractive index in left-handed materials, Physical Review Letters 85 (2000) 2933–2936.

[5] H. Chen, C. Chan, Acoustic cloaking in three dimensions using acoustic metamaterials, Applied Physics Letters 91 (2007) 183518.

[6] Z. Yang, J. Mei, M. Yang, N. Chan, P. Sheng, Membrane-type acoustic metamaterial with negative dynamic mass, Physical Review Letters 101(20) (2008) 204301.

[7] X. Zhou, G. Hu, Analytic model of elastic metamaterials with local resonances, Physical Review B 79 (2009) 195109.

[8] X. Liu, G. Hu, G. Huang, C. Sun, An elastic metamaterial with simultaneously negative mass density and bulk modulus, Applied Physics Letters 98 (2011) 251907.

[9] D. Del Vescovo, I. Giorgio, Dynamic problems for metamaterials : Review of existing models and ideas for further research, International Journal of Engineering Science 80 (2014) 153–172.

[10] R. Zhu, X. Liu, G. Hu, C. Sun, G. Huang, A chiral elastic metamaterial beam for broadband vibration suppression, Journal of Sound and Vibration 333 (2014) 2759–2773.

[11] X. Wang, H. Zhao, X. Luo, Z. Huang, Membrane-constrained acoustic metamaterials for low frequency sound insulation, Applied Physics Letters 108(4) (2016) 041905.

[12] R. E. Roberson, Synthesis of a nonlinear dynamic vibration absorber, Portions of a dissertation submitted to the Department of Applied Mechanics, Washington University, in partial fulfillment of the requirements for the degree of Doctor of Philosophy. (1952) 205–220.

[13] C. Soize, Vibration damping in low-frequency range due to structural complexity. A model based on the theory of fuzzy structures and model parameters estimation, Computers and Structures 58 (1995) 901–915.

[14] O. Gendelman, L. Manevitch, A. Vakakis, R. MĆloskey, Energy pumping in nonlinear mechanical oscillators : part I-dynamics of the underlying hamiltonian systems, Journal of Applied Mechanics 68 (2001) 34–41.

[15] A. Vakakis, O. Gendelman, Energy pumping in nonlinear mechanical oscillators : part II-resonance capture, Journal of Applied Mechanics 68 (2001) 42–48.

[16] A. Vakakis, Shock isolation through the use of nonlinear energy sinks, Journal of Vibration and Control 9 (2003) 79–93.

[17] G. Milton, M. Briane, J. Willis, On cloaking for elasticity and physical equations with a transformation invariant form, New Journal of Physics 8 (2006) 1–20.

[18] A. Carrella, M. Brennan, T. Waters, Static analysis of a passive vibration isolator with quasi-zero-stiffness characteristic, Journal of Sound and Vibration 301 (2007) 678–689.

[19] Z. Yang, H. Dai, N. Chan, G. Ma, P. Sheng, Acoustic metamaterial panels for sound attenuation in the 50-1000 Hz regime, Applied Physics Letters 96 (2010) 041906.

[20] Y. Xiao, J. Wen, X. Wen, Sound transmission loss of metamaterial-based thin plates with multiple subwavelength arrays of attached resonators, Journal of Sound and Vibration 331 (2012) 5408–5423.

[21] L. Viet, N. Nghi, On a nonlinear single-mass two-frequency pendulum tuned mass damper to reduce horizontal vibration, Engineering Structures 81 (2014) 175–180.

[22] R. Rubinstein, D. Kroese, Simulation and the Monte Carlo Method, Second Edition, John Wiley & Sons, 2008.

[23] A. Papoulis, Probability, Random Variables and Stochastic Processes, McGraw-Hill, New York, 1965.

[24] L. Guikhman, A. Skorokhod, The Theory of Stochastic Processes, Springer Verlag, 1979.

[25] M. Priestley, Spectral Analysis and Time Series, Academic Press, New York, 1981.

[26] M. Shinozuka, Simulation of multivariate and multidimensional random processes, Journal of the Acoustical Society America 49 (1971) 357–367.

[27] F. Poirion, C. Soize, Numerical methods and mathematical aspects for simulation of homogeneous and non homogeneous Gaussian vector fields, in : P. Krée, W. Wedig (Eds.), Probabilistic Methods in Applied Physics, Springer-Verlag, Berlin, 1995, pp. 17–53.

[28] L. Verlet, Computer "experiments" on classical fluids. I. Thermodynamical properties of Lennard-Jones molecules, Physical Review 159 (1) (1967) 98–103.

[29] E. Hairer, C. Lubich, G. Wanner, Geometric numerical integration illustrated by the Störmer/Verlet method, Acta Numerica 12 (2003) 399–450.

[30] C. Soize, I. E. Poloskov, Time-domain formulation in computational dynamics for linear viscoelastic media with model uncertainties and stochastic excitation, Computers and Mathematics with Applications 64 (11) (2012) 3594–3612.

[31] C. Desceliers, C. Soize, Non-linear viscoelastodynamic equations of three-dimensional rotating structures in finite displacement and finite element discretization, International Journal of Non-Linear Mechanics 39 (2004) 343–368.